Rotation Invariant Texture Analysis Using Radon and Fractional Fourier Transform

Fakhordin Mohammadi [1,2]
Junbin Gao[1]
Daming Shi[3]

[1]School of Computing and Mathematics, Charles Sturt University, Bathurst, NSW 2795, Australia
[2]Department of Mathematics, Hormozgan University, Bandarabbas, Iran
[3]School of Engineering and Information Sciences, Middlesex University, London NW4 4BT, UK
[1]f.mohammadi62@hotmail.com
[2]jbgao@csu.edu.au

Abstract. In this paper we propose a new rotation invariant feature descriptor for texture classification and clustering via first identifying the so-called principal direction of textures with the well-known Radon transform and then extracting features defined by the fractional Fourier transform of different order from the rotated textures along their principal direction. The performance of the proposed method is evaluated using different kind of texture sets. Results show the advantage of the proposed method over some existing algorithms.

Keywords: Texture classification, Radon transform, Fractional Fourier transform, Rotation invariant.

1 Introduction

Texture analysis plays an important role in image analysis, pattern recognition and machine vision. Texture-enriched modeling has become a powerful tool for content-based image retrieval and computer vision systems. Natural scenes consist of object surfaces exhibiting texture and a successful vision system should be able to deal with the textured world surrounding it. Texture is a ubiquitous visual experience. Texture can be used to characterize surfaces for a wide variety of real world objects or scenes such as terrain, fur, skin and minerals. In computer graphics and computer games, texture is employed to render synthetic images in order to reproduce the visual realism of the real world. Textures themselves can be acquired from a wide range of natural sources, e.g., scanning photographs. Different types of textures have different kind of advantages and disadvantages. Hand-drawn patterns pictures are aesthetically pleasing, however in some sense they lack photo-realism. For the application of most scanned images, the difficulties lie in avoiding visible seams or repetition when they are directly used for texture mapping. Today texture analysis methods have been widely used in many application areas. In remote sensing research, for example, texture analysis has played a major role in geographical analysis. Texture analysis approach has also found its way into other disciplines such as surface inspection [6, 29].

Texture analysis is important in many applications of computer image analysis for classification or segmentation of images based on local spatial variations of intensity or color. Like a conventional classification process, texture classification also involves two phases: the learning phase and the recognition phase. Both phases rely on a crucial pre-processing process in which one has to define and extract informative features from texture patterns. The ideal features should be invariant under as many transformations as possible. For example, it is very desirable for the extracted features to be translation-, scale- and rotation-invariant and also in-

sensitive to noise. Extracting and/or constructing such features is still a challenge facing researchers today. A wide variety of techniques for describing image texture have been proposed [29, 26]. Among many different kinds of texture classification approaches, statistical and model-based methods are widely used because of their capability of being applied to any type of texture. Feature learning or extraction is dominant among these approaches. There are many different feature extraction methods, from the features produced by some well-designed filters (e.g. Gabor filters and Wavelet filters) to the features incorporating global information on the textures (e.g Markov random field based texture features [32]). In a recent work [16], Khellah proposed a new approach to extract global image features for the purpose of texture classification by exploiting the idea from non-local denoising algorithm for image [3]. The proposed texture features are obtained by generating an estimated global map representing the measured intensity similarity between any given image pixel and its surrounding neighbors within a certain window.

People also are interested in extracting features which have certain geometric characterisation. Haralik et al. [10] first proposed the co-occurrence matrix method to get rotation-invariant texture features so that a classifier based on such features will be robust to texture rotation. Later, many rotation-invariant texture classification techniques were introduced and such features were used in texture classification problems. For example Kashyap and Khotanzed [15] used the rotation-invariant features based on a circular autoregressive model. In general, a rotation-invariant feature incorporates global information for a texture pattern. It is no surprise that Markov random fields can be used to construct rotation-invariant features [7, 8, 27]. The construction of another group of rotation-invariant features is based on filter bank responses. Wavelet packet was used in [19] to construct rotation-invariant feature for textures, while image histograms were employed in this process in [18]. Ojala et al. [23] proposed another efficient framework for rotation-invariant texture classification in which features are obtained from the histograms of the local binary patterns (LBPs). The LBP framework have been extended by many researchers, see [9, 11, 17, 20]. Based on the fact that the underlying textures are comprehensively described by their pixel joint probability density functions, an efficient density estimation for texture has been proposed in [17]. The LBP approach has wide applications, e.g., in face recognition [1] and dynamic texture recognition [30]. Furthermore, the work presented in [16] can be considered as extended LBP approach aiming at extracting

global image features for the purpose of texture classification by using dominant neighborhood structure.

In this paper we are still concerned with the rotation-invariant texture features. We aim to use the Radon transform and Fractional Fourier transform for deriving a rotation invariant texture classification method. In this method, the Radon transform is first employed to detect the principal direction of a texture. Then, the texture is rotated to place its principal direction at a reference direction, for example, the $0°$ direction. Fractional Fourier transform at several different orders are applied to the rotated texture to extract texture features. Experimental results show the superiority of the proposed approach compared with some existing methods.

The rest of this paper is organized as follows. In section 2 Radon transform and its application in finding the direction of the textures are reviewed. The Fractional Fourier transform and some of its useful properties is described in section 3. In Section 4, we present our rotation invariant texture classification algorithm. Experimental results are presented in Section 5 and finally conclusions are given in Section 6.

2 Texture Orientation

In this section, we will briefly review the Radon transform and its important properties, then we will describe the method of estimating the principal direction of textures via applying the Radon transform. The classical Radon transform projects an image along a radial line oriented at a specific angle. It transforms a 2-D image with lines into a domain of possible line parameters r and θ, where r is the smallest distance from the origin and θ is its angle with the x-axis. The Radon transform of 2-D image $\mathcal{R}_f$ (or simply $\mathcal{R}$) is defined as [12, 21, 28]:

$$\mathcal{R}(r,\theta)\left[f(x,y)\right] =$$
$$\int_{-\infty}^{\infty}\int_{-\infty}^{\infty}f(x,y)\delta(r-x\cos(\theta)-y\sin(\theta))dxdy \quad (1)$$

where $r = x\cos(\theta)+y\sin(\theta)$ is distance of a line from the origin, θ is the angle between the line and the y-axis and $\delta(.)$ is the Dirac function. It has been proved that the Radon transform has a very strong ability to capture information about curves and lines existing in a quite noisy image. The research has shown that such a property of Radon transform in extracting lines can be used to find the so-called principal direction for each texture. In fact, $\mathcal{R}(r,\theta)$ is roughly the information about the possible line angled at θ and displaced at r distance from the origin in the image f. The principal direction of a texture can be defined as the direction along

which there are more straight lines. In general some textures have no specific direction (isotropic textures) and some textures have one or more principal direction (anisotropic textures)[12, 21, 28].

Let us consider the definition of Radon transform for an image along different angles θ from $0°$ to $179°$ at a step size of $1°$. Suppose that the textures being considered are anisotropic. For a given angle θ_0, $\mathcal{R}(r, \theta_0)$ gives all the information about possible lines angled at θ_0 in a texture image. If the curve $\mathcal{R}(r, \theta_0)$ spreads well, we can imagine that more lines existing in the image along that direction θ_0. That means the variance of $\mathcal{R}(r, \theta_0)$ may be a good indicator of the line spreadness in the texture image. We are concerned with the principal orientation along which there are more straight lines, so the maxima θ_0 of the variance of Radon transforms would be the direction we are after. This idea was first investigated in [12] in which the maxima of the variance of Radon transform is used for estimating the principal direction of textures.

Mathematically we can work in the following way. First, to make the method isotropic, we chose a disk shape area (of radius r_0) in the middle of the texture and then the Radon transform is applied for this disk area at different angle $0°$ to $179°$ at a step size of $1°$. The variance of these transforms in different angels can be derived as

$$V_R(\theta) = Var\left(\mathcal{R}(r, \theta)\right), \qquad \theta \in [0, 180) \qquad (2)$$

The function $V_R(\theta)$ may have different local maxima in the interval $[0, 180)$ and consequently we have some different orientations in this interval. To identify a principal orientation from different local maxima and different directions we can calculate the second derivative of the variance function $V_R(\theta)$. Along the orientation that the second derivatives are minimum the variance changes more rapidly [12, 13]. Once we find the absolute maximum in the interval, we can estimate the principal direction of texture. To demonstrate this ability of Radon transform in estimating the principal direction of textures we present two different examples.

Example 1: Consider the texture sample (D68) from Brodatz album [2] that is rotated $20°$ anticlockwise, see Fig. 1(a). Fig. 2(b) shows the disk area selected in the middle of the texture. We applied the Radon transform for different angles from $0°$ to $179°$. Fig. 1(c) shows the variance function $V_R(\theta)$ for this transforms. As this figure shows the variance function has different local maxima. Fig. 1(d) shows the second derivative of the variance function along different angles. From this figure we can see there are
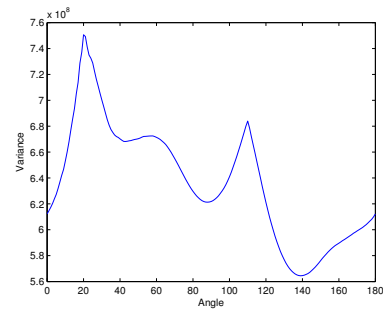
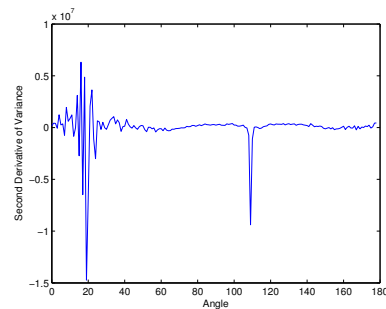**Figure 1:** Texture orientation for example 1
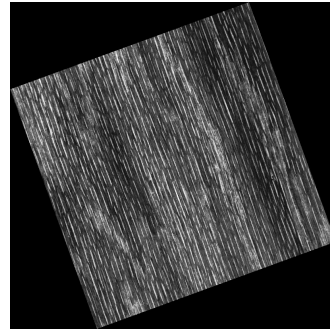
(a) Original texture
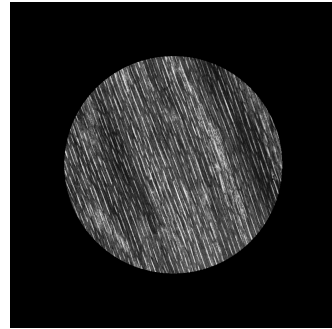
(b) Disk area of the texture

(c) The variance of projections

(d) Second derivative of variance

more straight lines along $20°$ and so this angle is the principal orientation.

Figure 2: Texture orientation for example 2

Example 2: Consider the texture sample (D101) from Brodatz album [2] that is rotated $60°$ anticlockwise, see Fig. 2(a). Fig. 2(a) and (b) show the original texture and the selected disk area in the middle of the texture. Fig. 2(c) and (d) show the variance function and its second derivative respectively. As shown in these figures, the variance of the projections has two local maxima. But there are more straight lines along $60°$ and so this angle is the principal orientation. This is identified by the plot of second derivatives of the variance in Fig. 2(d).

According to the above examples and the properties of Radon transform just described, the principal orientation of the texture can be estimated as follow

$$\alpha = \underset{\theta}{\operatorname{argmin}} \left(\frac{d^2 V_R(\theta)}{d\theta^2} \right) \tag{3}$$

where α is the principal orientation of the texture and $V_R(\theta)$ is the variance of the Radon projection of the disk area of the texture at the angle θ. This method for estimating the principal direction has good properties such as robustness to additive noise. For more details about this formula please see [12, 28].

3   Fractional Fourier Transform

In the classical Fourier transform (FT), the representation axis is changed from a representation in the (time) domain to a representation in the frequency domain, which corresponds to a counterclockwise rotation over an angle $\frac{\pi}{2}$ in the (t, ω)-plane. By applying FT twice we have

$$\mathcal{F}^2 f(t) = \mathcal{F}(\mathcal{F} f(t)) = f(-t) \tag{4}$$

Thus the representation axis is the reversed time axis, i.e., the time axis rotated over an angle π. In the similar way we have
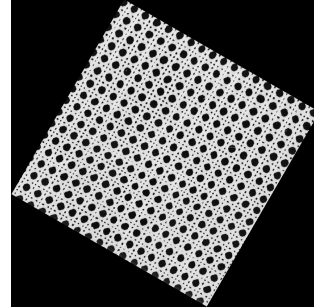
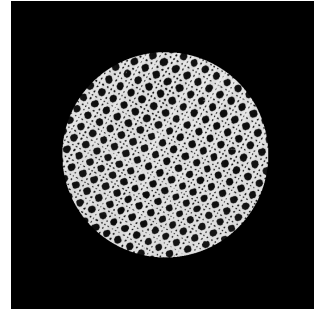$$\mathcal{F}^3 f(t) = \mathcal{F}(f(-t)) = F(-\omega) \tag{5}$$

and

$$\mathcal{F}^4 f(t) = \mathcal{F}(F(-\omega)) = f(t) \tag{6}$$

which are correspond to a rotation of the representation axis over $\frac{3\pi}{2}$ and 2π respectively. Thus the FT operator corresponds to a rotation in the time-frequency plane of the axis of representation over an angle $\frac{\pi}{2}$. Thus all the representations that one can obtain by the classical FT
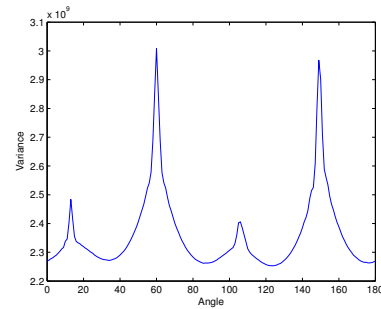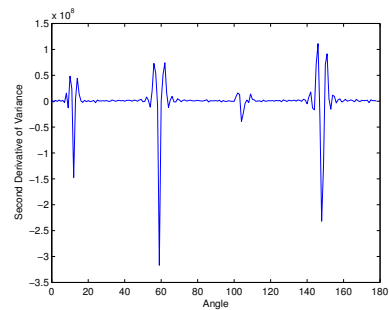

(a) Original texture

(b) Disk area of the texture

(c) The variance of projections

(d) Second derivative of variance

correspond to representations on the orthogonal axes of (t, ω) plane, possibly with a reversion of the orientation [4].

A generalization of the Fourier transforms to the so-called fractional Fourier transforms (FrFT) has been proposed by Namias in 1980 [22] and the FrFT has become a powerful tool for time-varying signal analysis [5, 25]. Like the classical FT corresponding to a rotation in the time frequency plane over an angle $\frac{\pi}{2}$, the FrFT will correspond to a rotation over an arbitrary angle $\frac{a\pi}{2}$ with a $a \in \mathbf{R}$.

Definition 3.1: The fractional Fourier transform of a function $f(t)$, with an angle $\alpha = \frac{a\pi}{2}$, is defined as

$$
\left(\mathcal{F}^{\alpha} f\right)(\omega) = \frac{e^{-i\left(\frac{\pi\hat{\alpha}}{4} - \frac{\alpha}{2}\right)} e^{\left(\frac{i}{2}\omega^2 \cot(\alpha)\right)}}{\sqrt{2\pi |\sin(\alpha)|}}
$$

$$
\times \int_{-\infty}^{\infty} e^{\left(\frac{-i\omega t}{\sin(\alpha)} + \frac{it^2 \cot(\alpha)}{2}\right)} f(t) dt \qquad (7)
$$

where $\hat{\alpha} = \operatorname{sgn}(\alpha)$ and $0 < |\alpha| < \pi$. For $\alpha = 0$ we have the identity operation $\left(\mathcal{F}^0 f\right)(\omega) = (\mathbf{I}f)(\omega) = f(\omega)$ and for $|\alpha| = \pi$ we define

$$
\left(\mathcal{F}^{\alpha} f\right)(\omega) = f(-\omega), \quad |\alpha| = \pi. \qquad (8)
$$

When $|\alpha| > \pi$, the definition is taken modulo 2 and reduced to the interval $|\alpha| \leq \pi$. For more details about this definition and its properties please see [4, 5, 25].

3.1   Discrete Fractional Fourier Transform

Similar to the ordinary FT, we need to consider how to calculate FrFT for discrete signals in applications. So this leads to the requirement of the discrete fractional Fourier transform (DFrFT). The discrete definition should be a discrete form of continuous definition in (7) and moreover it should be an extension of conventional discrete Fourier transform (DFT).

There are some different approaches to proposing the definition of DFrFT. Pie and et al. [25] proposed a definition for DFrFT based on orthogonal projection and Candan et al. [5] gave a definition based on a particular set of eigenvectors of the DFT matrix. In this paper we favor using the definition of DFrFT presented in [5]. The main point in this definition is to construct the eigenvalue decomposition of the discrete Fourier transform matrix $\mathbf{F}$.

Definition 3.2: let $f = [f_0, f_1, ..., f_{N-1}]^T$ be a discrete signal, the DFrFT of order α for the signal f is defined as

$$
\mathfrak{F}^{\alpha} f = \left(G \Lambda^{\alpha} G^T\right) f \qquad (9)
$$

where $\mathbf{F} = G \Lambda G^T$ is the eigenvalue decomposition of DFT matrix $\mathbf{F}$. For more details about the definition and the algorithm of the discrete fractional Fourier transform, we refer to [5, 24, 25].

4   Rotation Invariance Texture Feature Descriptors

The FrFT has become a powerful tool for time-varying signal analysis. However it is not rotation invariant and the FrFT changes significantly when the image is rotated. As mentioned in Section 2, Radon transform is a powerfull tool for detecting the orientations of a texture. So, by estimating the orientations of a textures, rotating along the principal direction and then applying the FrFT we can derive a rotation invariant method for cassifying textures. Fig 3 shows the proposed rotation invariant algorithm for texture classification. In this method, first a disk shape area from the middle of the image has been selected. Then by using Radon transform and the method mentioned in equation (3) the principal direction of the texture is estimated. The texture is rotated so that the principal direction moves to a reference direction such as $0°$. The FrFT of different orders is then applied to the rotated texture and finally the texture features can be extracted. It is worth to mention that while we select a disk area in the middle of textures, Radon transform for a texture is actually a shift and translation of the Radon transform of the original texture and so there is no need to compute the Radon transform for all rotated textures.

For the FrFT $I^{\alpha} = \mathfrak{F}^{\alpha} f$ of the order α, the following features are calculated

$$
e_1^{\alpha} = \frac{1}{MN} \sum_{i=1}^{M} \sum_{j=1}^{N} |I_{i,j}^{\alpha}|^2, \qquad (10)
$$

$$
e_2^{\alpha} = \frac{1}{MN} \sum_{i=1}^{M} \sum_{j=1}^{N} |I_{i,j}^{\alpha}|. \qquad (11)
$$

where M and N are the size of FrFT. In the above definition, $\mathbf{e}_1$ is the power spectrum while $\mathbf{e}_2$ is the absolute value of the real and imaginary parts of the FrFT.
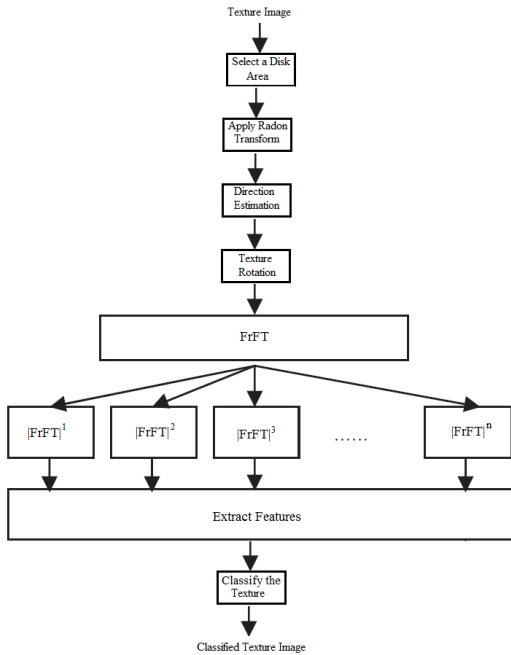
So by applying FrFT in a finite number of different orders $I^{\alpha_1}, I^{\alpha_2}, ..., I^{\alpha_n}$, feature vector e_1 and e_2 are calculated for a texture as follows

$$
\mathbf{e}_1 = \left(e_1^{\alpha_1}, e_1^{\alpha_2}, ..., e_1^{\alpha_n}\right), \qquad (12)
$$

$$
\mathbf{e}_2 = \left(e_2^{\alpha_1}, e_2^{\alpha_2}, ..., e_2^{\alpha_n}\right) \qquad (13)
$$

Then features is normalized by calculating the mean and variance within each vector. Finally for these features of many textures, a k-nearest neighbor (k-NN) classifier based on the Euclidean distance (Ed) is used to measure similarity between textures and to classify them.

Figure 3: The proposed a rotation invariant algorithm for texture classification.

Then each texture image is rotated 17 times from $10°$ to $180°$ with $10°$ increment in an anticlockwise direction to produce 17 new texture images. There are 17 variants plus the original image for each texture. So we create a dataset of total number of 80×18 texture images. For each image in this set by using the proposed method, we calculated the features e_1 and e_2 in (12) and (13) for $n = 10$. Training images are used as the standard images and then a k-NN classifier was employed to classify each texture based on the extracted features against the training images. For each feature the correct classification rate (CCR) is measured as follows:

$$CCR = \frac{c_0}{t_0} \times 100 \qquad (14)$$

where c_0 and t_0 is the total number of correctly classified textures and the total number of classified textures respectively. Table 1 provides the CCR of the proposed method for different features. As shown in this table, this method is very efficient for classifying the texture.

Figure 4: The 80 used textures from the Brodatz. 1th row: D1, D2, D3, D4, D5, D6, D8, D10, D11, D12. 2nd row: D13, D15, D18, D19, D20, D21, D22, D24, D25, D26. 3rd row: D27, D31, D34, D35, D36, D37, D46, D47, D49, D50. 4th row: D51, D52, D54, D57, D61, D62, D63, D64, D651, D66. 5th row: D67, D68, D69, D71, D73, D74, D75, D76, D78, D80. 6th row: D81, D83, D85, D86, D87, D88, D89, D90, D91, D92. 7th: D93, D94, D95, D96, D97, D98, D99, D100, D101, D102. 8th row: D103, D104, D105, D106, D107, D108, D109, D110, D111, D112

5 Experimental Results

In this section we conduct several experiments to demonstrate the potential of the newly constructed features in texture classification and clustering. The experimental results and the efficiency of the proposed method for texture classification and clustering will be analyzed.
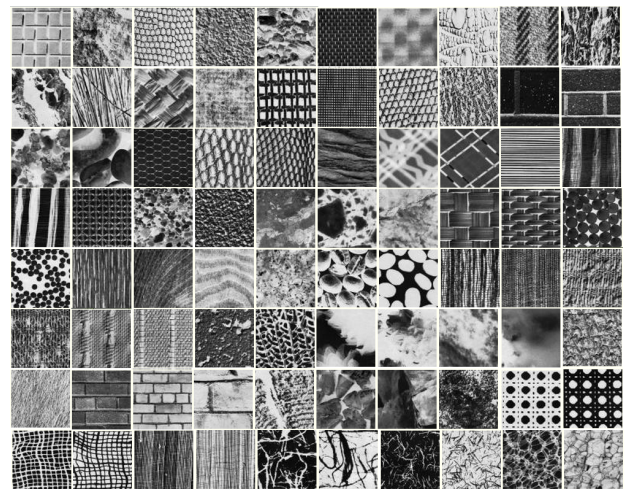
5.1 Experimental Setting

Experiments are carried out to demonstrate the capability of our method in texture image classification and clustering. We evaluate the efficiency of the proposed method on a dataset of 1440 texture images from the Brodatz standard texture album [2]. For our purpose, 80 different texture images of size 640×640 in the Brodatz texture library are selected as testing data. Some sample image textures are exhibited in Fig. 4.

5.2 Comparison with other methods

The results have also been compared with other similar existing methods for texture classification such as in Chen and Kundu [7], Khouzani and Zadeh [12], and the

Table 1: Correct Classification Rate (CCR)

	Features	
	e_1	e_2
CCR %	96.25%	97.50%

Table 2: Comparison between the results of the proposed methods and some of the methods from the literature

	Proposed Method	Methods from the literature
Textures in [7]	99.90%	95.00%
Textures in [12]	98.33%	96.70%
Textures in [14]	98.33%	99.90%

et al. [14]. For a fair comparison, we conducted our experiments according the experimental setting used in those above-mentioned methods. For example, particularly, we applied our method as done in Section 5.1 for the textures from Brodatz album that are used in [7]. We also applied the proposed method to the 60 textures that are used in [12] and [14]. Table 2 shows the comparison between the best result for proposed method and the best results of the method in these literatures. As results shown, our method is more accurate or comparable with these methods.

5.3 Clustering

To further demonstrate the capability of the new features e_1 and e_2 in clustering, we used these features to cluster randomly chosen 80 textures. For this purpose, we derived the features e_1 and e_2 for each texture for $n = 10$. So we have 80×2 feature vectors as follow:

$$\mathbf{e}_1^j, \ j = 1, 2, ..., 80; \tag{15}$$

$$\mathbf{e}_2^j, \ j = 1, 2, ..., 80. \tag{16}$$

Thus, for each texture, a vector $\mathbf{v}^j, \ j = 1, 2, ...80$ is constructed as follows

$$\mathbf{v}^j = [\mathbf{e}_1^j, \mathbf{e}_2^j], \ j = 1, 2, ..., 80. \tag{17}$$

Then a feature matrix V can be constructed with the $\mathbf{v}^j$ in the rows. We simply apply the Principal Component Analysis (PCA) to the matrix V, then a 2D-scatter plot for the textures based on two principal components of the features $\mathbf{e}_1$ and $\mathbf{e}_2$ can be drawn. Fig. 5 displays

Figure 5: Clustered textures using the features e_1 and e_2.
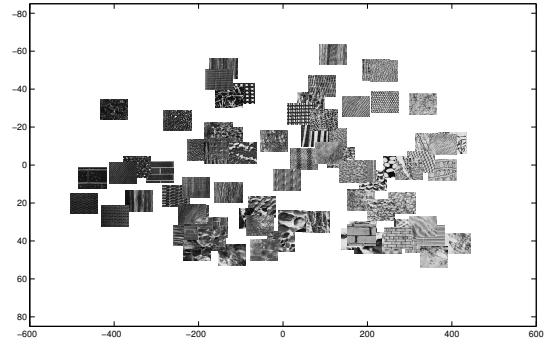
the scatter plot for the 80 textures based on the features $\mathbf{e}_1$ and $\mathbf{e}_2$ and their PCA coordinates. As shown in this figure the newly constructed features are efficient for texture clustering. From Fig. 5, it is clearly seen that the dark and bright texture images are separated well. Some texture clusters are also obvious, for example, on the left hand side of the picture, a cluster of dark brick-like textures stands out. Similarly another cluster of detailed texture patterns is revealed in the middle bottom area.

6 Conclusion

In this paper a rotation-invariant feature for texture analysis based on Radon transform and FrFT is proposed. In this method, the principal direction of a texture is estimated using Radon transform and then the image is rotated to place the principal direction at $0°$. Then FrFT of different orders is applied to extract the features for texture classification. Since this method use different orders of FrFT in extracting feature of each texture, it is very efficient in classifying different kind of texture. Experimental results show that this method is comparable to many other existing methods. Further investigation is needed, for example, how well the newly constructed is in terms of the state-of-the-art classifier such support vector machines.

References

[1] T. Ahonen, A. Hadid, and M. Pietikinen. Face description with local binary patterns: Application to face recognition. *IEEE Trans. Pattern Anal. Mach. Intell.*, 28(12):2037–2041, 2006.

[2] P. Brodatz. *Texture: A Photographic Album for Artists and Designers*. Dover Publications, New York, 1996.

[3] A. Buades, B. Coll, and J. Morel. A non-local algorithm for image denoising. In *IEEE Computer Society Conference on Computer Vision and Pattern Recognition*, volume 2, 2005.

[4] A. Bultheel and H. Martínez-Sulbaran. A shattered survey of the fractional Fourier transform. Manuscript, 2003.

[5] C. Candan, M.A. Kutay, and H.M. Ozaktas. The discrete fractional Fourier transform. *IEEE Trans. Signal Processing*, 48(5):1329–1337, 2000.

[6] C. H. Chen, L. F. Pau, P. S. P. Wang, and A. K. Jain. *The Handbook of Pattern Recognition and Computer Vision*. World Scientific Publishing Co., 2nd edition, 1998.

[7] J. Chen and A. Kundu. Rotation and gray scale transform invariant texture identification using wavelet decomposition and hidden markov model. *IEEE Trans. Pattern Anal. Mach. Intell.*, 16(2):208–214, 1994.

[8] H. Deng and D. A. Clausi. Gaussian MRF rotation-invariant features for image classification. *IEEE Trans. Image Processing*, 26(7):951–955, 2004.

[9] Z. Guo, L. Zhang, and D. Zhang. A completed modeling of local binary pattern operator for texture classification. *IEEE Trans. Image Processing*, 19(6):1657–1663, 2010.

[10] R. M. Haralik, K. Shanmugam, and I. Dinstein. Texture features for image classification, vol. smc-3, no. 6, pp. , jun., 1973. *IEEE Trans. Syst., Man Cybern.*, 3(6):610–621, 1973.

[11] X. Huang, S. Z. Li, and Y. Wang. Shape localization based on statistical method using extended local binary pattern. In *Proc. Int. Conf. Image Graphics*, pages 184–187, 2004.

[12] K. Jafari-Khouzani and H. Soltanian-Zadeh. Radon transform orientation estimation for rotation invariant texture analysis. *IEEE Trans. Pattern Anal. Mach. Intell.*, 27(6):1004–1008, 2005.

[13] K. Jafari-Khouzani and H. Soltanian-Zadeh. Rotation invariant multiresolution texture analysis using radon and wavelet transforms. *IEEE Trans. Image Processing*, 14(6):783–794, 2005.

[14] A. Jalil, T.A. Cheema, and A. Manzar. Rotation and gray-scale-invariant texture analysis using radon and differential Radon transforms based hidden Markov models. *IET Image Processing*, 4(1):42–48, 2009.

[15] R. Kashyap and A. Khotanzed. A model-based method for rotation invariant texture classification. *IEEE Trans. Pattern Anal. Mach. Intell.*, 8(4):472–481, 1986.

[16] F. M. Khellah. Texture classification using dominant neighborhood structure. *IEEE Trans. Image Process*, 20(11):3270–3279, 2011.

[17] H. Lategahn, S. Gross, T. Stehle, and T. Aach. Texture classification by modeling joint distributions of local patterns with Gaussian mixtures. *IEEE Trans. Image Processing*, 19(6):1548–1557, 2010.

[18] L. Li, C. S. Tong, and S. K. Choy. Texture classification using refined histogram. *IEEE Trans. Image Processing*, 19(7):1371–1378, 2010.

[19] A. Liane and J. Fan. Texture classification by wavelet packet signature. *IEEE Trans. Pattern Anal. Mach. Intell.*, 15(11):1186–1191, 1993.

[20] S. Liao, M. W. K. Law, and A. C. S. Chung. Dominant local binary patterns for texture classification. *IEEE Trans. Image Processing*, 18(5):1107–1118, 2009.

[21] Y. Liu. Edge detection based on localized Radon transform. In *Proceedings of IEEE International Symposium on Geoscience and Remote Sensing*, pages 3675–3678, 2005.

[22] V. Namias. The fractional order Fourier transform and its application to quantum mechanics. *J. Inst. Math. Applicat.*, 25:241–265, 1980.

[23] T. Ojala, M. Pietikainen, and T. Maenpaa. Multiresolution gray-scale and rotation invariant texture classification with local binary patterns. *IEEE Trans. Pattern Anal. Mach. Intell.*, 24(7):971–987, 2002.

[24] S.C. Pei and M.H. Yeh. Improved discrete fractional Fourier transform. *Optics Letters*, 22:1047–1049, 1997.

[25] S.C. Pei, M.H. Yeh, and C.C. Tseng. Discrete fractional Fourier transform based on orthogonal projections. *IEEE Trans. Signal Processing*, 47(5):1335–1348, 1999.

[26] Jing Yi Tou, Yong Haur Tay, and Phooi Yee Lau. Recent trends in texture classification: A Review. In *Proceedings of Symposium on Progress in Information & Communication Technology*, pages 63–68, 2009.

[27] M. Varma and A. Zisserman. A statistical approach to material classification using image patch exemplars. *IEEE Transactions on Pattern Analysis and Machine Intelligence*, 31(11):2032–2047, 2009.

[28] Y. Wang, Y. Lei, and J. Huang. An image copy detection scheme based on radon. In *Proceedings of 2010 IEEE 17th International Conference on Image Processing*, Hong Kong, 2010.

[29] J. Zhang and T. Tan. Brief review of invariant texture analysis methods. *Pattern Recognition*, 35:735–747, 2002.

[30] G. Zhao and M. Pietikinen. Dynamic texture recognition using local binary patterns with an application to facial expressions. *IEEE Trans. Pattern Anal. Mach. Intell.*, 27(6):915–928, 2007.

[31] Y. Zhao, L. Zhang, P. Li, and B. Huang. Classification of high spatial resolution imagery using improved gaussian markov random-field-based texture features. *IEEE Trans on Geoscience and Remote Sensing*, 45(5):1458–1468, 2007.

[32] http://www.ux.uis.no/$\sim tranden/brodatz.html$